The GPRI Multi-mode Differential Interferometric Radar for Ground-based Observations

Charles Werner, Gamma Remote Sensing, CH-3073 Gümligen, Switzerland
Andreas Wiesmann, Gamma Remote Sensing, CH-3073 Gümligen, Switzerland
Tazio Strozzi, Gamma Remote Sensing, CH-3073 Gümligen, Switzerland,
Rafael Caduff, Gamma Remote Sensing, CH-3073 Gümligen, Switzerland,
Andrew Kos, Terrarsense AG, CH-9470 Werdenberg, Switzerland
Urs Wegmüller, Gamma Remote Sensing, CH-3073 Gümligen, Switzerland

Abstract

We describe the Gamma Portable Radar Interferometer (GPRI) designed to perform in-situ measurements of motion along the line of sight (LOS) using differential interferometric techniques. Using this capability it is possible to generate DEMs, and measure surface deformation < 0.2mm. Results from test cases are shown including the Aletsch Glacier and the Kornhaus Bridge in Bern. Ground-based interferometric observations are complementary to spaceborne or airborne SAR based measurements because they can be acquired continuously and processed to mitigate the effects of temporal decorrelation and atmospheric phase variability.

1 Introduction

The Gamma Portable Radar Interferometer (GPRI) developed by Gamma Remote Sensing is a multi-mode FM-CW radar operating at 17.2 GHz, shown in Figure 1. The system is fully coherent and can be used to perform interferometric measurement of target motion along the line of sight (LOS). The radar has an operational range from 20 meters to 10 km. Compared with spaceborne or airborne radar systems, ground-based observations have flexibility in the selection of the imaging geometry to optimize visibility and sensitivity. Other advantages include the capability for frequent repeat observations to unambiguously track rapidly moving features, higher sensitivity to motion along the LOS due to the shorter wavelength, and the ability to acquire multiple observations to improve SNR and mitigate path delay variations due to tropospheric water vapour.

Figure 1: GPRI Instrument looking down on the Aletsch Glacier on 27-Jun-2011.

1 Instrument Description

The radar consists of an antenna tower mounted onto a computer-controlled azimuthal scanner. The antenna tower supports the transmitting antenna and two receiving antennas to form an interferometric array with a 25 cm vertical baseline. The RF electronics are contained in an enclosure mounted on the tower. Power and control is provided by the instrument computer and power supply located in a weatherproof enclosure located near the tower base. Baseband signals are digitized by a dual-channel software-defined radio (SDR) system located in the instrument computer enclosure. A GPS receiver located on the tower provides frequency and time reference for the GPRI and permits simultaneous operation of multiple GPRI instruments.

The GPRI uses 2.06 meter slotted-waveguide antennas to generate a fan-beam that is 0.4 degrees in azimuth x 35 degrees in elevation. During image acquisition, the radar performs a rotary scan of the scene at a programmable rate between 0.5 and 10 degrees/sec scan-

ning the scene line by line. Time required to obtain a single image is approximately 20 s for a 180 degree azimuthal sweep. Azimuth resolution is proportional to range with a value of 8.0 meters at 1 km distance. Differential motion of 8.715 mm results in 2π radians of differential phase between observations. The phase noise for a differential interferogram generated from two single-look complex (SLC) images is given by [1]:

$$\sigma_\phi = \frac{1}{\sqrt{SNR}}$$

Table 1 shows the relationship between SNR of the SLCs and standard deviation of the motion measurement.

SNR (dB)	σ_ϕ (deg.)	σ_r (mm)
30	1.81	0.044
20	5.73	0.139
10	18.1	0.438

Table 1: Single-Look Standard Deviation of Path Length Measurement with the GPRI

The FM-CW waveform used by the GPRI is generated by direct-digital synthesis (DDS) at baseband (100-300 MHz) with a programmable pulse rate between 100-4000 Hz. The DDS chirp waveform is heterodyned to 17.1 to 17.3 GHz in two steps with an intermediate frequency (IF) of 900-1100 MHz. Transmitter output power is approximately 100 mW.

The receiver front-end consists of a cavity filter and isolator followed by a low-noise amplifier. An IQ quadrature mixer is used to heterodyne the input signal down to the 900-1100 MHz IF. The FM chirp deramp is performed after amplification of the received signal in the 900-1100 MHz IF. An active bandpass filter amplifies the deramp mixer output in the filter passband of .025 to 2.8 MHz. Each channel is digitized using 16-bits/sample at an effective rate of 6.25 MHz. Separate receivers are used for the upper and lower antennas.

2 Radar Data Processing

FM-CW radar raw data require a an FFT to obtain a range profile [2]. The digitized echoes are processed using azimuth presumming, nominally 5:1 to improve the signal to noise ratio (SNR). The measured radar half-power range resolution is 0.94 meters while the antenna has a measured azimuth beamwidth of 0.46 degrees. The range-compressed chirp does not exhibit spreading due to chirp frequency non-linearity. The range and azimuth point target peak sidelobe levels are -28 dB in both range and azimuth.

3 Data Acquisition Modes

In order to perform interferometric measurements of target motion it is necessary that the scatters remain coherent during the measurement period. Making sequential measurements with short intervals decreases temporal decorrelation and minimizes phase shifts due to motion. This improves the measurement accuracy and is a significant of ground-based interferometric radar. Depending on the deformation rates of the target scene, different strategies for measurement are necessary.

3.1 DEM Generation

Interferograms for production of digital elevation models can be obtained by interfering measurements from the GPRI upper and lower receiving channels [3]. These DEMs can be used for visualization of the deformation data using a projection that corresponds to the visual view from above or from the radar location.

Since many interferograms from the upper and lower antennas can be obtained in a single deployment it is advantageous to average the individual interferograms to improve the SNR. There is little or no temporal decorrelation in these interferograms since the data are acquired simultaneously over a short time interval (< 20ms). The interferometric phase is dependent on the path difference between the upper and lower antennas and is a direct function of elevation angle and slant range. The interferometric phase can be converted to DEM heights by unwrapping the phase, combined with knowledge of the radar position and the altitude of a single point in the scene. The interferometric phase for an upper-lower interferogram combined with the radar intensity is shown in Figure 2.

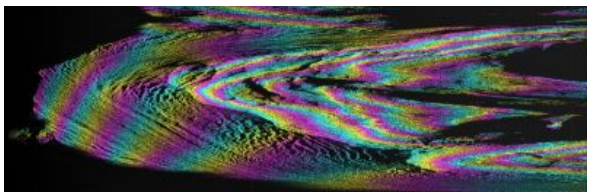

Figure 2: Interferogram from upper and lower antennas with 25 cm baseline.

Figure 2 was acquired at the Aletsch Glacier as viewed from the Bettmerhorn (see Figure 1). The interferogram is presented in polar format with the azimuth scan angle along the vertical edge and slant-range increasing from left to right. Each fringe represents 8.71 mm path difference between the signals received by the upper and lower antennas.

3.2 Deformation rates cm/day

Deforming features such as glaciers or mine walls have rates in the range of cm to meters/day. In this mode the radar is deployed at a single site and measures continuously at intervals between 1 an 10 minutes such that the deformation does not exceed several mm between observations. Typically a time series of N-1 interferograms is calculated from pairs of measurements (1,2), (2,3), (N-1, N). This sequence minimizes both temporal decorrelation, and the deformation phase to improve phase unwrapping accuracy.

From the set of differential interferograms an average deformation rate can be calculated by stacking of the individual differential interferograms.

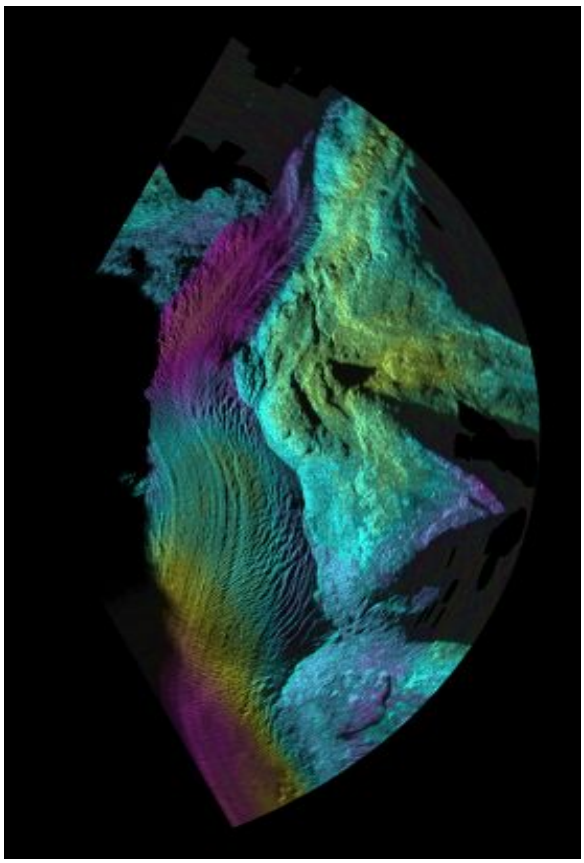

Figure 3: Aletsch glacier average deformation rate, color cycle 150 m/year LOS

The result of stacking 73 differential interferograms acquired over 4 hours with 3 minute interval at the Aletsch glacier indicates a maximum deformation rate of 150 meters LOS (Figure 3). The observed phase signals on the mountains are due to residual atmospheric path variablity. The observed glacier velocities are consistent with the results of Strozzi et al. [4] obtained by TerraSAR-X feature tracking.

3.2 Deformation rates cm/year

Observation of slowly moving features such as rock falls, landslides or tectonic displacement requires multiple measurement campaigns since very little motion occurs on a single day. On each day measurements should be acquired for several hours to minimize the variability in the atmospheric path delay as well as improve the SNR. An important issue with this type of measurement is that the radar antennas must be repositioned to within about 1 cm or better of the original position. This is necessary in order to minimize the interferometric phase component due to terrain height. A permanent pedestal is recommended for this type of measurement.

An example of this type of approach is given for the Aletschwald landslide on the slope adjacent to the Aletsch Glacier. The landslide was observed using both TerraSAR-X and the GPRI. TerraSAR-X observations were performed on 11-Jun-2011 and 25-Jul-2011. GPRI observations occurred on 27-Jun-2011 and 10-Aug-2011 from the opposite flank of the glacier valley. Each fringe of the TerraSAR-X image represents 15.6 mm of motion LOS. The terrain geocoded images of LOS deformation are shown in Figure 4 and Figure 5. Note that the GPRI data have higher spatial resolution and sensitivity to deformation.

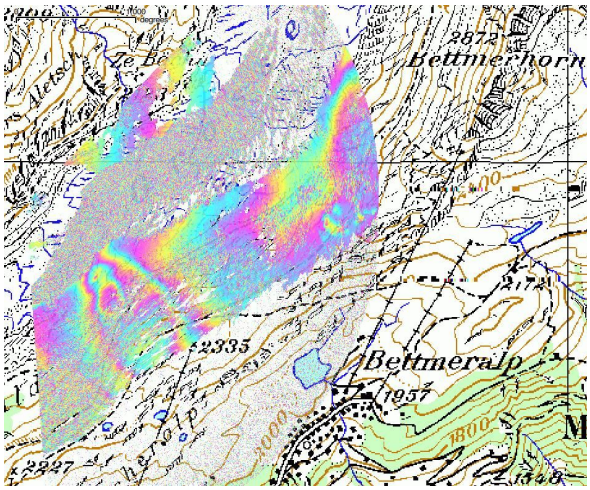

Figure 4: GPRI observation of the Aletschwald between 27-Jun-2011 and 10-Aug-2011

3.3 Deformation rates > cm/minute

The GPRI has the capability to make continuous high-rate deformation measurements while looking in fixed direction at rates of up to 4 kHz. This permits continuous deformation measurements of structures such as bridges and even the surface velocity of rivers. Figure 6 shows a tram traversing the Kornhaus bridge during a campaign on 1-Jul-2011.

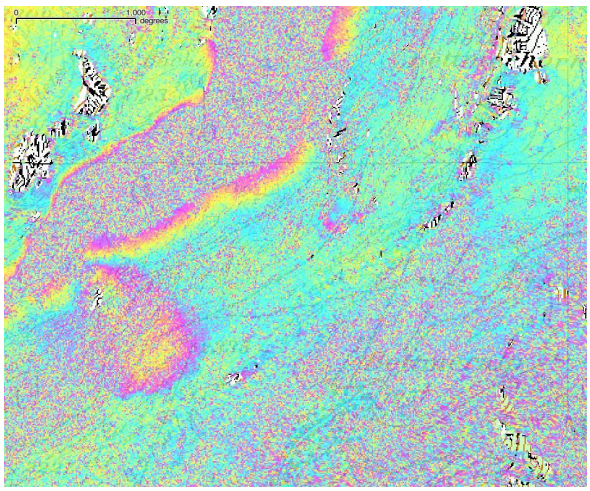

Figure 5: TerraSAR-X deformation along the LOS from 11-Jun-2011 to 25-Jul-2011

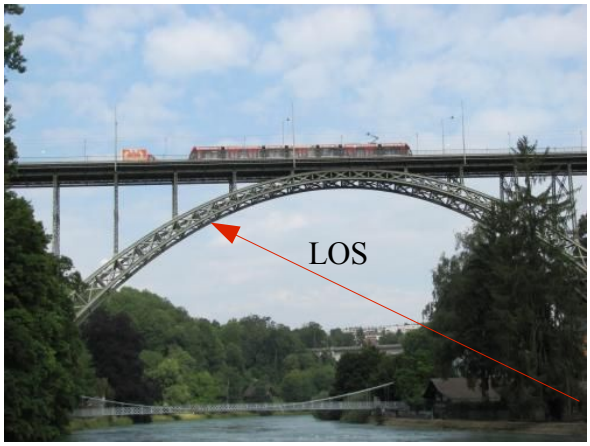

Figure 6: Tram traversing the Kornhaus bridge in Bern from right to left. The GPRI is under the bridge on the right bank.

The GPRI was located under the bridge looking up at an elevation angle of 40 degrees from the right river bank. Deformation measurements were performed at a 2 kHz sample rate. Figure 7 shows the interferometric deformation phase during the traversal indicating deformation of up to 6 mm along the LOS. Initial deformation of the road bed was away from the radar (up) followed by motion towards the radar (down) as the tram depressed the road bed.

Conclusions

We describe the GPRI and show a number of measurement scenarios to measure deformation along the LOS and generate interferometric DEMs. The short measurement intervals possible with ground-based radar extends the range of possible applications for differential interferometry to include rapidly deforming features such as glaciers and infrastructure.

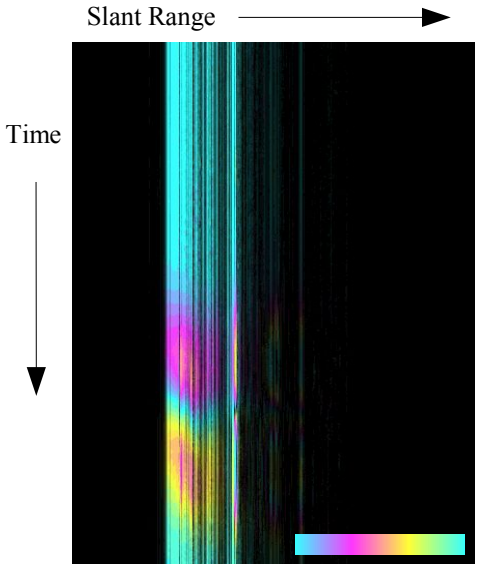

Figure 7: Kornhaus bridge deformation phase along the LOS for a 30 second observation period. Colour cycle = 8.71 mm motion.

References

[1]Dainty, J.C. (Editor), "Laser Speckle and Related Phenomenon",pp.29-35,Springer-Verlag, Berlin, 1984

[2]Carrara, W.G. Et all "Spotlight Synthetic Aperture Radar", pp 27-30. Boston, Artech House Inc. 1995

[3]Strozzi, T. C. Werner, A. Wiesmann, and U. Wegmüller, "Topography mapping with a portable real-aperture radar interferometer", accepted for publication in IEEE Geoscience and Remote Sensing Letters.

[4] Strozzi, T., R. Delaloye, H. Raetzo, U. Wegmüller, C. Werner and A. Wiesmann, "Survey of Landslide Activity, Rock Glacier Movement and Surface Glacier Velocity", Proceedings of the 4th TSX Science Team Meeting, DLR Oberpfaffenhofen, Germany, 14-16 February 2011", see http://sss.terrasar-x.dlr.de/

[5]Strozzi, T., R. Delaloye, A. Kääb, C. Ambrosi, E. Perruchoud, and U. Wegmüller, "Combined observations of rock mass movements using satellite SAR interferometry, differential GPS, airborne digital photogrammetry, and airborne photography interpretation," Journal of Geophysical Research, 115, F01014, doi:10.1029/2009JF001311, 2010.

Acknowledgements

Development is supported through the Swiss initiative to foster and promote Swiss scientific and technological competences related to space activities by the Swiss Space Office of the Swiss State Secretariat for Education and Research (contract A2310.0441). TerraSAR-X data © DLR (2011) provided under the DORIS FP7 project.